# Ground motion sample size vs estimation uncertainty in seismic risk

Georgios Baltzopoulos
*Assistant Professor, Dept. of Structures for Engineering and Architecture, Università degli studi di Napoli Federico II, Naples, Italy*

Iunio Iervolino
*Full Professor, Dept. of Structures for Engineering and Architecture, Università degli studi di Napoli Federico II, Naples, Italy*

Roberto Baraschino
*PhD Candidate, Dept. of Civil Engineering, National Technical University of Athens, Athens, Greece*

ABSTRACT: In the context of seismic risk assessment as per the performance-based earthquake engineering paradigm, a probabilistic description of structural vulnerability is often obtained via dynamic analysis of a non-linear numerical model. It typically involves subjecting the structural model to a suite of ground-motions that are representative, as a sample, of possible seismic shaking at the site of interest. The analyses' results are used to calibrate a stochastic model describing structural response as a function of seismic intensity. The sample size of ground motion records used is, nowadays, usually governed by computation-time constraints; on the other hand, it directly affects the estimation uncertainty which is inherent in risk analysis carried out in this way. Recent studies have suggested methodologies for the quantification of estimation uncertainty, to be used as tools for determining the appropriate number of records for each application on an objective basis. The present study uses one of these simulation-based methodologies, based on standard statistical inference methods and the derivation of structural fragility via incremental dynamic analysis, to investigate the accuracy of the risk estimate (e.g., the annual failure rate) vs the size of ground motion samples. These investigations consider various scalar intensity measures and confirm that that the number of records required to achieve a given level of accuracy for annual failure rate depends not only on the dispersion of structural responses, but also on the shape of the hazard curve at the site. This indicates that the efficiency of some frequently-used intensity measures is not only structure-specific but also site-specific.

## 1. INTRODUCTION

Performance-based earthquake engineering (PBEE; Cornell and Krawinkler 2000), entails the probabilistic quantification of structure-specific seismic risk. This risk can be quantified by the annual rate of earthquakes able to cause the structure to violate a seismic performance objective, which can be simply termed the failure rate, $\lambda_f$, given by Eq. (1):

$$\lambda_f = \int_{im} P\left[f \left| im \right.\right] \cdot \left| d\lambda_{im} \right| \qquad (1)$$

where the conditional probability term $P\left[f \left| im \right.\right]$ represents what is often known as a fragility function, which provides the probability of failure for various values of a seismic intensity measure (IM), while $\lambda_{im}$ is the annual rate of earthquakes exceeding the value of shaking intensity *im* and therefore constitutes a measure of seismic hazard at the site.

The state-of-the-art in PBEE is to analytically estimate structure-specific fragility functions by means of procedures that require multiple dynamic analysis runs of a numerical model of the structure. These analyses typically use a multitude of acceleration records as input motion, in order to map the record-to-record variability of inelastic structural response (Shome et al. 1998). On the other hand, the evaluation of $\lambda_{im}$ for various intensity levels, which is known as the hazard curve, is usually obtained by means of

probabilistic seismic hazard analysis (PSHA; e.g., McGuire 1995), which typically employs empirical ground motion prediction models (GMPMs) to account for the attenuation of shaking intensity.

In modern practice, the number of records used for non-linear dynamic analysis of a structure is typically limited due to the large computation times required for running intricate structural models at high non-linearity levels. However, this number of records determines the sample-size of seismic structural responses that is used for fragility estimation and, eventually, the failure rate. Since these descriptors of seismic fragility and risk are inferred from finite-size samples, they are only estimates of the corresponding true values, and are therefore affected by estimation uncertainty (Iervolino 2017). In fact, the estimator of $\lambda_f$, obtained using a specific sample of ground motions and denoted using a hat symbol as $\hat{\lambda}_f$, can be regarded as a random variable (RV) whose distribution is a function of the sample size. In other words, computing $\hat{\lambda}_f$ over and over for a number of times using different sets of accelerograms (equal in number to the first one and equivalent in characteristics) would lead to a different value for the estimator each time around. Although GMPMs are also based on samples of recorded ground motion, these datasets are extensive enough to allow the assumption that the estimation uncertainty underlying $\hat{\lambda}_f$ is only due to the fragility portion of Eq. (1).

Estimation uncertainty present in parametric fragility models fitted from dynamic analysis results has also been highlighted by other past studies (Eads et al. 2015; Gehl et al. 2015; Jalayer et al. 2015): in fact, a quantitative measure of the effect of this uncertainty on the failure rate, can be obtained according to Eq. (2):

$$CoV_{\hat{\lambda}_f} = \frac{\sqrt{VAR\left[\hat{\lambda}_f\right]}}{E\left[\hat{\lambda}_f\right]} = \frac{\Delta}{\sqrt{n}} \qquad (2)$$

where the notation $CoV_{\hat{\lambda}_f}$ indicates the coefficient of variation of $\hat{\lambda}_f$, $VAR\left[\hat{\lambda}_f\right]$ and $E\left[\hat{\lambda}_f\right]$ denote its variance and expected value, respectively, $n$ is the sample size of accelerograms used to estimate the fragility function and $\Delta$ is a parameter that depends on the so-called *efficiency* of the IM chosen to express structural fragility and also on the shape of the site-specific hazard curve.

The objective of the present article is to employ a simulation-based methodology for the quantification of estimation uncertainty, which was recently proposed as part of a broader-in-scope study (Baltzopoulos et al. 2018a) and investigate the efficiency of some commonly-used scalar IMs, directly in terms of the ground motion sample size required to contain the mean relative estimation error, rather than in terms of its frequently-used proxy; i.e., the dispersion of response. This methodology is based on incremental dynamic analysis (IDA; Vamvatsikos and Cornell 2001) and involves using a relatively large set of accelerograms to run dynamic analyses for an assortment of simple inelastic structures. The results of these analyses are then used to fuel a procedure based on Monte-Carlo simulation, where fragility estimates at various limit states and using alternative IMs are generated and statistics of the estimator of the failure rate, $\hat{\lambda}_f$, are extracted.

The structure of this article follows this order: first there is a brief presentation of the methodology for estimating structural fragility via an IM-based procedure and of that for obtaining statistics of the estimator of failure rate. Then specific applications are given, considering single-degree-of-freedom (SDOF) and simple frame structures exposed to a variety of seismic hazard conditions. Finally, the issue of record sample size vs estimation uncertainty in the estimate of the risk metric is discussed, in conjunction with the choice of IM used as interfacing variable, followed by some concluding remarks.

## 2. METHODOLOGY

In order to investigate the issue of ground motion sample-size vs estimation uncertainty, fragility is derived via dynamic analysis using the so-called IM-based approach using IDA. IDA consists of running a series of analyses for a non-linear structure, using a suite of accelerograms that are scaled in amplitude in order to represent a broad range of IM levels. At each IM level, a measure of structural response is registered generically named an engineering demand parameter (EDP). An exception to this are cases where response approaches numerical instability, which translates to lack of convergence in the computer model (Shome and Cornell 2000). Thus, at the conclusion of the dynamic analyses at an adequate number of IM levels, a quasi-continuous EDP-IM relationship is obtained, termed an IDA curve (Figure 1).

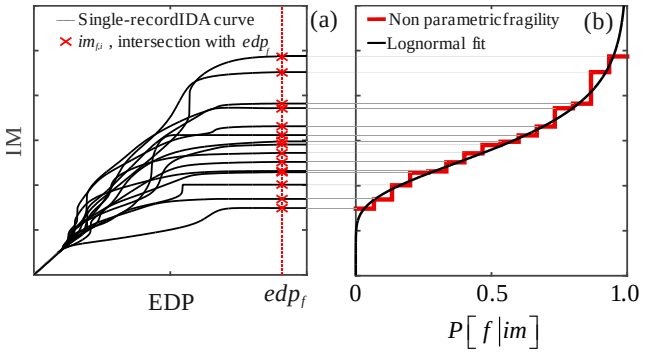


*Figure 1: IM-based derivation of seismic fragility via incremental dynamic analysis. Set of generic IDA curves and intersections of each curve with a vertical line passing from the failure threshold (a); parametric (lognormal) and non-parametric representations of the fragility function derived from the IDA results (b).*

It can be assumed that violation of some limit state of seismic performance (i.e., failure) occurs whenever the EDP response exceeds a certain threshold value, denoted as $edp_f$. In this context, IM-based fragility entails the introduction of an additional RV, $IM_f$, which is the lowest seismic intensity that a record has to be scaled to, in order to cause $EDP > edp_f$. Thus, $IM_f$ may be viewed as the seismic intensity that causes structural failure and, consequently, the fragility function can be defined as the complementary cumulative distribution function of $IM_f$ i.e., $P[f|im] = P[IM_f \le im]$.

In the context of IDA, the lowest IM value for each record that causes the structure to reach the performance threshold, can be calculated by finding the height, $im_{f,i}$, where the i-th IDA curve intersects the vertical line $EDP = edp_f$, $i = \{1, 2, ..., n\}$, $n$ being the total number of records), as shown in Figure 1a. These values can be considered as a sample of realizations of $IM_f$ and, consequently, well-known statistical methods (e.g., Baker 2015) can be used to fit a parametric probability distribution model to that sample. One frequently-used distribution is the lognormal (Figure 1b), which is completely defined by two parameters: the logarithmic mean and standard deviation, whose point estimates based on one sample, $\hat{\eta}_{IM_f}$ and $\hat{\beta}_{IM_f}$ respectively, are given in Eq.(3):

$$\begin{cases} P[f|im] = \Phi\left[\left(\log im - \hat{\eta}_{IM_f}\right)/\hat{\beta}_{IM_f}\right] \\ \hat{\eta}_{IM_f} = 1/n \cdot \sum_{i=1}^{n} \log\left(im_{f,i}\right) \\ \hat{\beta}_{IM_f} = \sqrt{1/(n-1) \cdot \sum_{i=1}^{n}\left[\log\left(im_{f,i}\right) - \hat{\eta}_{IM_f}\right]^2} \end{cases} \quad (3)$$

where $im_{f,i}$ is the i-th record's (lowest) scaled IM value causing failure and $\Phi(\cdot)$ is the standard (cumulative) Gaussian function. A non-parametric alternative is to assume that the observed sample values approximate the fragility by defining a stepwise function, according to Eq.(4):

$$P[f|im] = P[IM_f \le im] = \frac{1}{n} \cdot \sum_{i=1}^{n} I_{(im_{f,i} \le im)} \quad (4)$$

where $I_{(im_{f,i} \le im)}$ is an indicator function that returns 1 if $im_{f,i} \le im$ and 0 otherwise. In either case, once the fragility function has been estimated, the point estimate of the failure rate $\hat{\lambda}_f$ can be obtained via Eq. (1).

As already mentioned, the estimation uncertainty inherent in deriving the fragility from a finite sample of structural responses is propagated to the estimator of seismic risk $\hat{\lambda}_f$, which should be therefore regarded as a RV and a function of the sample: assuming that one were to perform a number of different IDAs, using each time a set of accelerograms of the same size but with different records than the previous ones, it is to be expected that the estimated fragility curve will differ from time to time, thus leading to different estimates of the failure rate (i.e., different realizations of the RV $\hat{\lambda}_f$).

One way of quantifying the estimation uncertainty of $\hat{\lambda}_f$ is by means of the mean relative estimation error, $CoV_{\hat{\lambda}_f}$, which can be regarded as the coefficient of variation of the estimator. In the case of IM-based fragility via IDA, the relationship between $CoV_{\hat{\lambda}_f}$ and the ground motion sample size $n$ can be approximated by means of Monte-Carlo simulation (Baltzopoulos et al. 2018a). This procedure begins with a reference IDA that uses a relatively large amount of records ($n = 200$ is used herein) to derive a reference fragility function, which can be either lognormal or non-parametric. The simulation entails randomly sampling $s$ times from this reference distribution of $IM_f$ for different sample sizes $n = \{2,3,...,200\}$ (in the case of non-parametric, empirical fragility, this translates to resampling with substitution). At the next step in the procedure, either new lognormal fragility curves are fitted to each extracted sample according to Eq.(3), or Eq.(4) is mustered to directly express the fragility function. In either case, integrating the fragility with a hazard curve, according to Eq.(1), leads to a point estimate of the failure rate at the j-th simulation, denoted $\hat{\lambda}_{f,j}$. As a last step, after $s$ simulations have been concluded at any given record sample size $n$, $E\left[\hat{\lambda}_f\right]$ and $VAR\left[\hat{\lambda}_f\right]$ can be approximated via the first two moments of the Monte-Carlo-generated sample of point estimates. By substituting these values into Eq.(2), one obtains Eq.(5):

$$CoV_{\hat{\lambda}_f} \approx \frac{\sqrt{\frac{1}{s-1}\cdot\sum_{j=1}^{s}\left(\hat{\lambda}_{f,j}-\frac{1}{s}\cdot\sum_{k=1}^{s}\hat{\lambda}_{f,k}\right)^2}}{\frac{1}{s}\cdot\sum_{j=1}^{s}\hat{\lambda}_{f,j}} \quad (5)$$

which provides the simulation-based approximation for $CoV_{\hat{\lambda}_f}$.

## 3. APPLICATIONS

The methodology outlined in the previous sections is applied to an assortment of simple inelastic structures, which are assumed to be located at three Italian sites that can be considered representative of varying levels of seismic hazard severity. The three sites considered are in the vicinity of the cities of L'Aquila (representative of a high seismic hazard site), Naples (medium hazard levels) and Milan (low hazard) and are all assumed to be characterized by firm soil conditions. At each of the three sites a yielding single-degree-of-freedom system is considered, with natural vibration period $T = 0.7$ s and viscous damping ratio $\zeta = 0.05$. Additionally, at the L'Aquila site a four-story steel moment-resisting frame is considered, with first mode period $T_1 = 1.82$ s.

Hazard curves were calculated at these sites, in terms of several different scalar IMs, using the software REASSESS (Chioccarelli et al. 2018) employing the seismic source model from Meletti et al. (2008). Hazard was obtained at all three sites for spectral pseudo-acceleration at the SDOFs' period, $Sa(T = 0.7\text{ s})$, and also for peak ground acceleration (PGA) and $Sa(T = 1.8\text{ s})$ at L'Aquila. Also considered, were two more advanced IMs that implicitly account for spectral shape (Bojórquez and Iervolino 2011; Eads et al. 2015), namely average spectral acceleration $S_{avg}$ and $I_{Np}$, given by Eqs.(6) and (7), respectively:

$$S_{avg} = \sqrt[n_T]{\prod_{i=1}^{n_T}\left[Sa(T_i)\right]} \quad (6)$$

$$I_{Np} = Sa(T_1)\cdot\left[S_{avg}/Sa(T_1)\right]^{0.40} \quad (7)$$

where $n_T$ is the number of periods, $T_i$, that are used in the definition of $S_{avg}$. Hazard curves in terms of $S_{avg}$ and $I_{Np}$ are obtained at all three sites using $T_i = \{0.7\text{s}, 1.0\text{s}, 1.5\text{s}\}$ for the seismic risk assessment of the SDOF structures and at L'Aquila, using $T_i = \{0.6\text{s}, 1.8\text{s}, 2.5\text{s}, 4.0\text{s}\}$ for that of the steel frame. These hazard curves are shown in Figure 2.

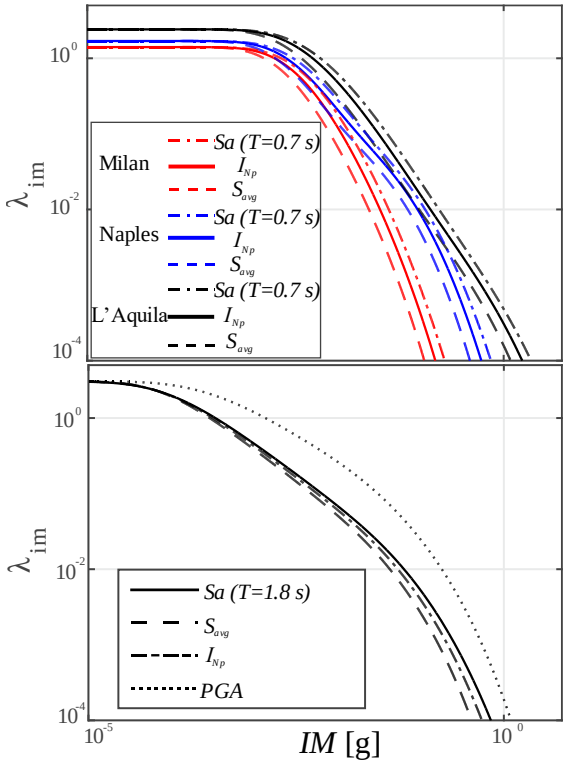


*Figure 2: Annual exceedance rates (hazard curves) at the three Italian sites for all IMs considered; hazard curves used for seismic risk assessment of the SDOF structures (above) and for the four-story steel frame presumed at L'Aquila (below).*

In order to construct reference fragility functions for all of the structures considered, via IDA, a set of two-hundred records was selected from the NESS flatfile (Pacor et al. 2018), avoiding records that were likely affected by near-source effects such as rupture directivity or by site effects due to deformable soil deposits.

### *3.1. SDOF structures*

The simplest structures used in this application are yielding SDOF systems that follow a peak-oriented hysteretic rule (Lignos and Krawinkler 2011) that also considers in-cycle strength degradation by including a softening, negative-stiffness post-peak branch in their monotonic pushover (backbone) curve, thus permitting explicit consideration of the collapse limit state in the numerical analyses. The yield threshold and backbone characteristics of the three SDOF oscillators have been tweaked to render them ostensibly risk-equivalent; i.e., they were determined so that each structure at its presumed site exhibits the same estimated annual collapse rate ( $\hat{\lambda}_f \approx 3.6\cdot10^{-4}$ ) when fragility at collapse is calculated from the IDA flat-lines (Vamvatsikos and Cornell 2004) with $n = 200$ records, using $S_{avg}$ as IM. The numerical model of the oscillators and IDA analyses were set up in the OPENSeeS analysis platform (McKenna 2011) using the DYANAS interface (Baltzopoulos et al. 2018b). Both lognormal models and non-parametric representations are considered for collapse fragilities.

In Figure 3, the resulting values of the relative mean estimation error $CoV_{\hat{\lambda}_f}$ from the Monte-Carlo simulation procedure – i.e., from Eq.(5) – are plotted against record sample size $n$ for all combinations of IM, structure-site pairing and fragility model (eighteen cases in total), also reporting the point estimates of $\hat{\lambda}_f$ at $n = 200$ in the legend. It is clear that these two-hundred-record estimates shift when switching IM, but this is mainly an effect of how sensitive structural response is to seismological parameters when records are scaled (Luco and Cornell 2007), and not directly related to ground motion sample size and estimation uncertainty. The figure also reports the number of records required to limit $CoV_{\hat{\lambda}_f}$ to

20% and 10% for some cases. The most immediate observation emanating from Figure 3, is that, for risk-wise nominally equivalent structures that express fragility in terms of the same IM, the shape of the hazard curve makes a difference on the number of records required to limit estimation uncertainty to a desired level, as verified also analytically in the past (Baltzopoulos et al. 2018a). The parameter $\Delta$, that summarizes the combined effect of the shape of the hazard curve and IM efficiency on the coefficient of variation of $\hat{\lambda}_f$ according to Eq. (2), can be evaluated by means of a least-squares fit of that equation to the simulation data and is given in Table 1.

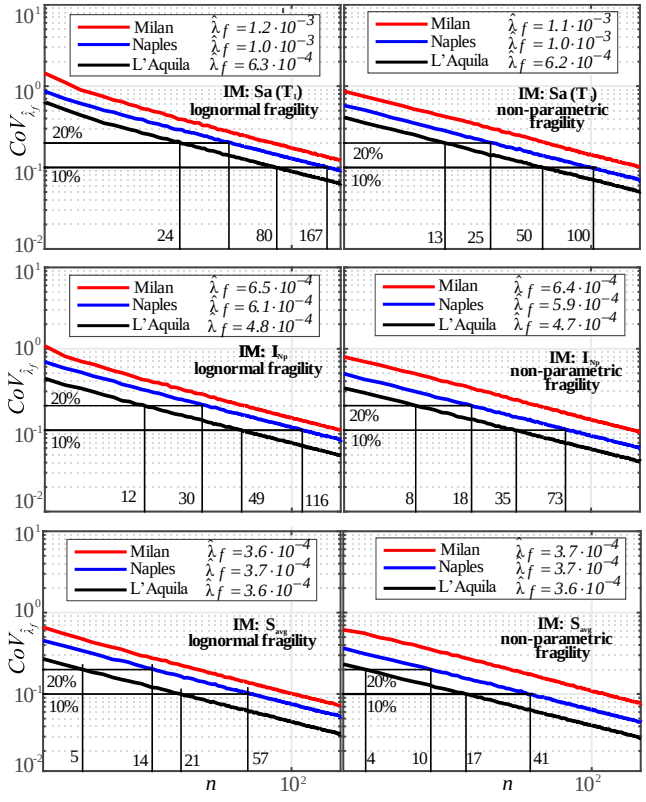


*Figure 3: Mean relative estimation error, $CoV_{\hat{\lambda}_f}$, calculated via Monte Carlo simulation for the three SDOF structures considered, plotted against ground motion sample size $n$.*

### *3.2. MDOF steel frame structure*

For the MDOF structure, that is the steel moment-resisting frame presumed built at the higher-hazard-level location of L'Aquila, the same procedure was followed as for the three simpler SDOF systems. In this case, a center-line, non-linear finite-element model of the structure created in the OPENSeeS environment was used to run IDA using the same two-hundred record set. Differently from the previous applications, the collapse limit state was not considered; instead, fragility was derived for two generic limit states whose violation can be conventionally defined by exceedance of some threshold in terms of maximum inter-story drift ratio, $(IDR)$: $IDR > 1.5\%$ was considered for the first limit state and $IDR > 2.5\%$ for the second. As in the previous case, the simulation-based values of $CoV_{\hat{\lambda}_f}$ were calculated for $n = \{2, 3, ..., 200\}$ using all four IMs for which hazard curves had been derived and the results are plotted in Figure 4. The corresponding $\Delta$ values, i.e., the site-and-structure-specific parameter that allows the mean relative estimation error to be expressed as a function of record sample size as $CoV_{\hat{\lambda}_f} = \Delta/\sqrt{n}$, is also reported in Table 1.

### *3.3. Discussion of the results*

A cursory examination of the results from the two examples, already reveals that adoption of a traditional IM such as PGA, can be inadequate for risk analysis of a flexible structure, since the number of records required to limit $CoV_{\hat{\lambda}_f}$ to an (arbitrary) value as low as 10% verges on the impracticable. In certain cases, such as the case of estimating annual collapse rate and especially at low-seismicity areas, the same can be said even for first mode spectral acceleration $Sa(T_1)$; in fact, even for these simple inelastic structures, the number of records required to limit the mean relative estimation error below 10% exceeds fifty.

Finally, it is interesting to compare the relative efficiency of the geometric mean spectral acceleration $S_{avg}$ vs $I_{Np}$, the weighted geometric mean; i.e., compare their ability to reduce estimation uncertainty for a fixed record sample

size. From the calculated $\Delta$ values, it can be observed that, for these specific applications, $I_{Np}$ is somewhat more efficient than $S_{avg}$ at limit states corresponding to lower level of inelasticity, while $S_{avg}$ overcomes $I_{Np}$ in efficiency near collapse. More elaborate discussion of the issue can be found in the article from which this study was inspired (Baltzopoulos et al. 2018a).

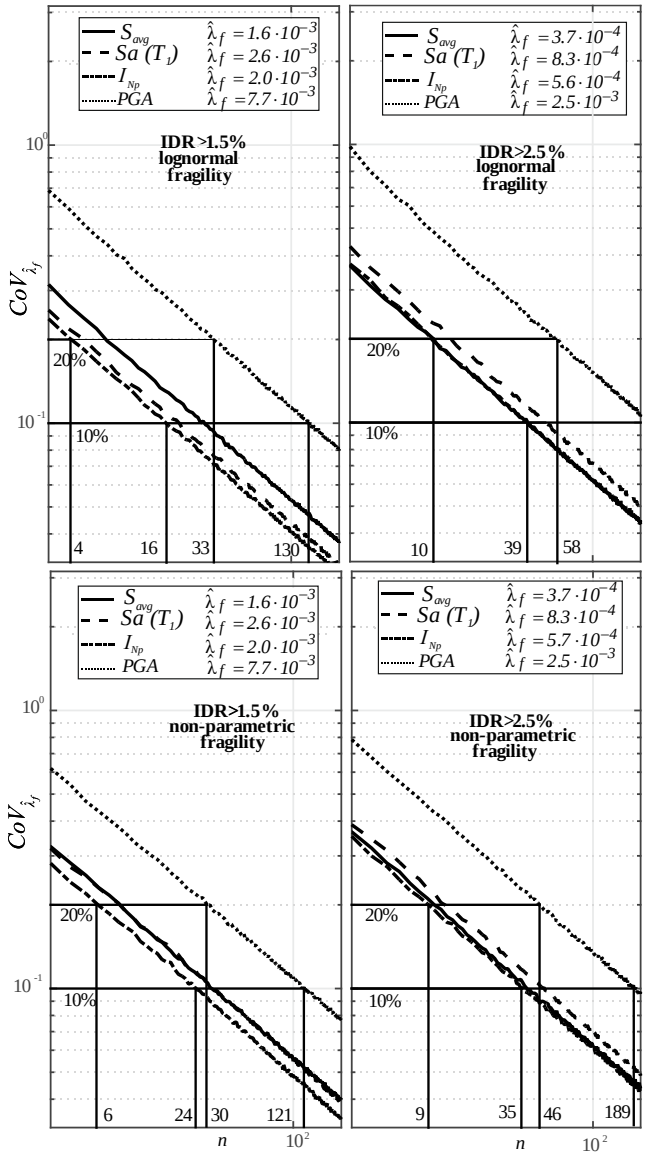


*Figure 4 : Mean relative estimation error, calculated via Monte Carlo simulation for the steel frame assumed at L'Aquila, plotted against ground motion sample size $n$ .*

*Table 1: Dispersion of intensity causing failure and site-/structure- specific parameter $\Delta$ of the mean relative estimation error ( $CoV_{\hat{\lambda}_f} = \Delta/\sqrt{n}$ ),provided for each site, structure, IM, limit state and assumption about the fragility function (LogN – lognormal, Emp - empirical).*

| Site | Stru-cture | Limit State | IM | $\beta_{IM_f}$ | Fragi-lity | $\Delta$ |
|---|---|---|---|---|---|---|
| L'Aquila | Four-story steel moment resisting frame $T_1$=1.82s | IDR>1.5% | PGA | 0.608 | LogN | 1.148 |
| | | | | | Emp | 1.078 |
| | | | $Sa(T_1)$ | 0.253 | LogN | 0.438 |
| | | | | | Emp | 0.561 |
| | | | $I_{Np}$ | 0.220 | LogN | 0.408 |
| | | | | | Emp | 0.490 |
| | | | $S_{avg}$ | 0.265 | LogN | 0.530 |
| | | | | | Emp | 0.563 |
| | | IDR>2.5% | PGA | 0.639 | LogN | 1.536 |
| | | | | | Emp | 1.357 |
| | | | $Sa(T_1)$ | 0.333 | LogN | 0.715 |
| | | | | | Emp | 0.694 |
| | | | $I_{Np}$ | 0.267 | LogN | 0.628 |
| | | | | | Emp | 0.605 |
| | | | $S_{avg}$ | 0.241 | LogN | 0.622 |
| | | | | | Emp | 0.628 |
| Milan | Inelastic SDOF (T=0.70s) | Collapse | Sa(T) | 0.475 | LogN | 1.839 |
| | | | | | Emp | 1.476 |
| Naples | | | | 0.444 | LogN | 1.318 |
| | | | | | Emp | 0.998 |
| L'Aquila | | | | 0.441 | LogN | 0.922 |
| | | | | | Emp | 0.712 |
| Milan | | | $I_{Np}$ | 0.378 | LogN | 1.468 |
| | | | | | Emp | 1.383 |
| Naples | | | | 0.341 | LogN | 1.099 |
| | | | | | Emp | 0.855 |
| L'Aquila | | | | 0.337 | LogN | 0.701 |
| | | | | | Emp | 0.580 |
| Milan | | | $S_{avg}$ | 0.273 | LogN | 1.039 |
| | | | | | Emp | 1.119 |
| Naples | | | | 0.223 | LogN | 0.760 |
| | | | | | Emp | 0.641 |
| L'Aquila | | | | 0.214 | LogN | 0.457 |
| | | | | | Emp | 0.409 |

## 4. CONCLUSIONS

The introduction of ever more realistic, and thus complex, numerical structural models in probabilistic seismic risk analysis, renders the topic of constraining the appropriate size of the input ground motion set to use, ever topical. This study builds on recent proposals to base the determination of the number of records on the notion of limiting estimation uncertainty of the risk metric to desired levels. A general rule-of-thumb emerging from these results, is that using record sample sizes in the thirty-to-fifty range, in combination with adoption of more advanced,

efficient IMs, tends to keep the mean relative estimation error at 10% or below. The higher end of that range is needed for cases that combined limit states corresponding to larger inelastic excursions with site subjected to lower hazard levels. It became apparent that the so-called efficiency of seismic intensity measures, i.e., their ability to keep estimation uncertainty to the desired levels using smaller-size samples of ground motions, is in fact site- and structure-dependent, as recent research has shown.

## 5. ACKNOWLEDGEMENTS

The study presented in this paper was developed within the activities of ReLUIS (Rete dei Laboratori Universitari di Ingegneria Sismica) for the project ReLUIS-DPC 2014–2018, as well as within the H2020-MSCA-RISE-2015 research project EXCHANGE-Risk (Grant Agreement Number 691213).

## 6. REFERENCES

Baker, J. W. (2015). "Efficient analytical fragility function fitting using dynamic structural analysis." *Earthquake Spectra*, 31(1).

Baltzopoulos, G., Baraschino, R., and Iervolino, I. (2018a). "On the number of records for structural risk estimation in PBEE." *Earthquake Engineering & Structural Dynamics*, (In press).

Baltzopoulos, G., Baraschino, R., Iervolino, I., and Vamvatsikos, D. (2018b). "Dynamic analysis of single-degree-of-freedom systems (DYANAS): a graphical user interface for OpenSees." *Engineering Structures*, 177, 395–408.

Bojórquez, E., and Iervolino, I. (2011). "Spectral shape proxies and nonlinear structural response." *Soil Dynamics and Earthquake Engineering*, 31(7), 996–1008.

Chioccarelli, E., Cito, P., Iervolino, I., and Giorgio, M. (2018). "REASSESS V2.0: software for single- and multi-site probabilistic seismic hazard analysis." *Bulletin of Earthquake Engineering*, (in press).

Cornell, C. A., and Krawinkler, H. (2000). "Progress and Challenges in Seismic Performance Assessment." *PEER Center News*, 3(2), 1–4.

Eads, L., Miranda, E., and Lignos, D. G. (2015). "Average spectral acceleration as an intensity measure for collapse risk assessment." *Earthquake Engineering and Structural Dynamics*, 44(12), 2057–2073.

Gehl, P., Douglas, J., and Seyedi, D. M. (2015). "Influence of the number of dynamic analyses on the accuracy of structural response estimates." *Earthquake Spectra*, 31(1).

Iervolino, I. (2017). "Assessing uncertainty in estimation of seismic response for PBEE." *Earthquake Engineering & Structural Dynamics*, 46(10), 1711–1723.

Jalayer, F., De Risi, R., and Manfredi, G. (2015). "Bayesian Cloud Analysis: Efficient structural fragility assessment using linear regression." *Bulletin of Earthquake Engineering*, 13(4), 1183–1203.

Lignos, D. G., and Krawinkler, H. (2011). "Deterioration Modeling of Steel Components in Support of Collapse Prediction of Steel Moment Frames under Earthquake Loading." *Journal of Structural Engineering*, 137(11), 1291–1302.

Luco, N., and Cornell, C. A. (2007). "Structure-specific scalar intensity measures for near-source and ordinary earthquake ground motions." *Earthquake Spectra*, 23(2), 357–392.

McGuire, R. K. (1995). "Probabilistic Seismic Hazard Analysis and Design Earthquakes: Closing the Loop." *Bulletin of the Seismological Society of America*, 85(5), 1275–1284.

McKenna, F. (2011). "OpenSees: A framework for earthquake engineering simulation." *Computing in Science and Engineering*, 13(4), 58–66.

Meletti, C., Galadini, F., Valensise, G., Stucchi, M., Basili, R., Barba, S., Vannucci, G., and Boschi, E. (2008). "A seismic source zone model for the seismic hazard assessment of the Italian territory." *Tectonophysics*, 450(1–4), 85–108.

Pacor, F., Felicetta, C., Lanzano, G., Sgobba, S., Puglia, R., D'Amico, M., Russo, E., Baltzopoulos, G., and Iervolino, I. (2018). "NESS v1.0: A worldwide collection of strong-motion data to investigate near source effects." *Seismological Research Letters*.

Shome, N., and Cornell, C. A. (2000). "Structural seismic demand analysis: Consideration of collapse." *8th ACSE Specialty Conference on Probabilistic Mechanics and Structural Reliability*, (3), PMC2000-119.

Shome, N., Cornell, C. A., Bazzurro, P., and Carballo, J. E. (1998). "Earthquakes, records, and nonlinear responses." *Earthquake Spectra*, 14(3), 469–500.

Vamvatsikos, D., and Cornell, C. A. (2001). "Incremental Dynamic Analysis." *Earthquake Engineering and Structural Dynamics*, 31(3), 491–514.

Vamvatsikos, D., and Cornell, C. A. (2004). "Applied incremental dynamic analysis." *Earthquake Spectra*, 20(2), 523–553.